XIX IMEKO World Congress
Fundamental and Applied Metrology
September 6−11, 2009, Lisbon, Portugal

# VIRTUAL CAPACITANCE METER BASED ON IMPEDANCE MODULUS MEASUREMENT

*Artur Skórkowski* [1], *Adam Cichy* [2]

[1] Silesian University of Technology, Institute of Measurement Science, Electronics and Control, Gliwice, Poland, artur.skorkowski@polsl.pl
[2] Silesian University of Technology, Institute of Measurement Science, Electronics and Control, Gliwice, Poland, adam.cichy@polsl.pl

**Abstract** – The capacitance can be calculated from the impedance modulus value of the object under test. It is possible, if a two-terminal network is represented by a series connection of a resistor and a capacitor and the reactance of the capacitor is considerably greater than the resistance (e.g. in a low-loss capacitor). In this case the error of the approximation can be omitted. A virtual realization of such meter has been presented in the paper. This one shows the idea of the signal processing in the quasi-balanced circuit. Quasi-balanced circuits are the AC circuits designated for impedance component measurements. Similar as the balanced circuits, the quasi-balanced circuits have a special status called a quasi-balance status. This is usually a phase shift between two selected signals of the circuits. The circuit is driven to the quasi-balance status by controlling of only one variable element and then the value of the measured impedance component can be calculated using the adjusted value of the variable element. The meter has been built with the application of the data acquisition card USB NI-6009, which has been controlled by a software programmed in the LabVIEW environment.

**Keywords**: capacitance measurement, quasi-balanced circuits.

## 1. INTRODUCTION

Modulus impedance measurements are performed in practice rather exceptionally. In some cases however such measurement can be good choice. E. g. if under test is an impedance object of significantly different components (as a capacitor with a small dielectric loss factor or an inductor with a small *Q* factor) instead of the main impedance component the impedance modulus can be measured. In such case the application of a quasi-balanced circuit can be regarded. The method first was implemented in a quasi-balanced passive measuring circuits. Now the method is implemented also in active measuring circuits [1, 2], but more and more frequently also in virtual circuits [5, 6].

The quasi-balanced circuits for impedance component measurements have several advantageous features. Contrary to circuits using the balanced method the convergence problem is absent when the quasi-balance method is used. The circuit equilibrium state there is achieved by means of setting only one control element. What's more: 1° the sensitivity of quasi-balanced circuit grows with frequency decrease, 2° no inductive elements are needed in the circuit structure, so it can be used for measurements in the VLF frequency band (several hertz or even parts of hertz), 3° algorithmic phase-sensitive detectors allow to shorten the detection time to sub-multiple of the signal period. The measurement in the quasi-balanced circuit needs a significantly shorter measuring time in comparison with other measuring methods.

An implementation of the quasi-balance method for the capacitance measurement is presented in the paper. Particularly instead of the capacitance the impedance modulus is measured by the use of programmed processing of the measurement signals. Main aim of the work was checking of the measurement idea. Preliminary test results will be used for the circuit construction designed for a impedance modulus measurement in the VLF frequency band.

## 2. ERROR OF THE MEASUREMENT METHOD

The real capacitance value is connected with the imaginary component $\operatorname{Im}\underline{Z}_X$ of the impedance $\underline{Z}_X$ under test. If the series equivalent circuit RC represents the object, the following equation defines the capacitance to be measured:

$$C = \left| \frac{1}{\omega \operatorname{Im}\underline{Z}_X} \right| . \tag{1}$$

The capacitance value $\hat{C}$ calculated from the impedance modulus $|\underline{Z}_X|$ equals to:

$$\hat{C} = \frac{1}{\omega |\underline{Z}_X|} . \tag{2}$$

The calculation of the capacitance value from the equation (2) instead of (1) yields a relative error:

$$e_r(C) = \frac{\hat{C} - C}{C} = \frac{\frac{1}{\omega|\underline{Z}_X|} - \frac{1}{\omega \operatorname{Im}\underline{Z}_X}}{\frac{1}{\omega \operatorname{Im}\underline{Z}_X}} = \frac{\operatorname{Im}\underline{Z}_X}{|\underline{Z}_X|} - 1 . \tag{3}$$

Impedance modulus is bound with the impedance components by the following equation:

$$\left|\underline{Z}_X\right|^2 = \left[\mathrm{Re}\,\underline{Z}_X\right]^2 + \left[\mathrm{Im}\,\underline{Z}_X\right]^2 . \tag{4}$$

The equation (4) can be written in the form:

$$\left|\underline{Z}_X\right|^2 = \left(\mathrm{Im}\,\underline{Z}_X\right)^2 \left[\left(\frac{\mathrm{Re}\,\underline{Z}_X}{\mathrm{Im}\,\underline{Z}_X}\right)^2 + 1\right]. \tag{5}$$

Taking into account the definition of the dielectric loss factor $\tan\delta$:

$$\tan\delta = \frac{\mathrm{Re}\,\underline{Z}_X}{\mathrm{Im}\,\underline{Z}_X} \tag{6}$$

the equation (3) of the error caused by the capacitance calculation from the approximate equation (2), can be written in the form:

$$e_r(C) = \frac{1}{\sqrt{1+\tan^2\delta}} - 1 . \tag{7}$$

The curve of the relative error vs. the dielectric loss factor $\tan\delta$ is shown in the Fig. 1.

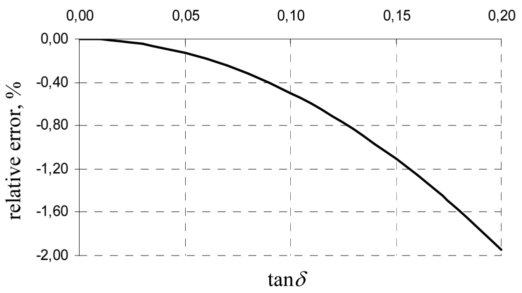


Fig. 1. The relative error of the capacitance measurement result versus the dielectric loss factor $\tan\delta$ of the capacitor.

The relative error of the capacitance calculation caused by the approximation of the impedance imaginary component by the impedance modulus should be less than accepted limit value $\varepsilon$:

$$\left|e_r(C)\right| \le \varepsilon . \tag{8}$$

Putting (7) into (8) there is obtained:

$$\left|\frac{1}{\sqrt{1+\tan^2\delta}} - 1\right| \le \varepsilon . \tag{9}$$

Because $\tan\delta > 0$ (so the denominator is always bigger than 1), then

$$\left|\frac{1}{\sqrt{1+\tan^2\delta}} - 1\right| = 1 - \frac{1}{\sqrt{1+\tan^2\delta}} . \tag{10}$$

The condition (9) can be written in the form:

$$1 - \frac{1}{\sqrt{1+\tan^2\delta}} \le \varepsilon , \tag{11}$$

From (11) results the following condition:

$$\tan\delta \le \frac{\sqrt{\varepsilon(2-\varepsilon)}}{1-\varepsilon} . \tag{12}$$

## 3. QUASI-BALANCED CIRCUIT FOR MEASUREMENT OF IMPEDANCE COMPONENTS

The essential structure of the quasi-balanced circuit for the impedance modulus measurement is shown in the Fig. 2.

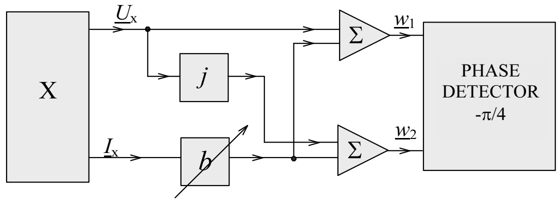


Fig. 2. A block diagram of the quasi-balanced circuit for the measurement of the impedance modulus.

The block X contains the impedance $\underline{Z}_X$ under test and supplying circuits (a generator). Measuring output signals are respectively: $\underline{U}_X$ – voltage drop thorough impedance under test, and $\underline{I}_X$ – the current flowing thorough this impedance. Signals $\underline{U}_X$ and $\underline{I}_X$ are processed according to the diagram presented in the Fig. 2. Signals $\underline{w}_1$ and $\underline{w}_2$ on the phase-sensitive detector inputs are described by equations:

$$\begin{cases} \underline{w}_1 = \underline{U}_X + b\underline{I}_X \\ \underline{w}_2 = j\underline{U}_X + b\underline{I}_X \end{cases} . \tag{13}$$

The quasi-balance state of the circuit consists in a phase shift angle between the signals $\underline{w}_1$ and $\underline{w}_2$ equals to $-\pi/4$. This state is described by the condition:

$$Arg\left(\frac{\underline{w}_1}{\underline{w}_2}\right) = -\frac{\pi}{4} . \tag{14}$$

From (14) results the following equation:

$$\mathrm{Re}\left(\frac{\underline{w}_1}{\underline{w}_2}\right) = -\mathrm{Im}\left(\frac{\underline{w}_1}{\underline{w}_2}\right). \tag{15}$$

The ratio of the distinguished signals $\underline{w}_1$ and $\underline{w}_2$ is bound with the measured impedance:

$$\frac{\underline{w}_1}{\underline{w}_2} = \frac{\underline{U}_X + b\underline{I}_X}{j\underline{U}_X + b\underline{I}_X} = \frac{\dfrac{\underline{U}_X}{\underline{I}_X} + b}{j\dfrac{\underline{U}_X}{\underline{I}_X} + b} = \frac{\underline{Z}_X + b}{j\underline{Z}_X + b} . \tag{16}$$

After conversion of the (16) the following equation there is obtained:

$$\frac{\underline{w}_1}{\underline{w}_2} = \frac{-j\left|\underline{Z}_X\right|^2 - jb\operatorname{Re}\underline{Z}_X - b\operatorname{Im}\underline{Z}_X}{\left|j\underline{Z}_X + b\right|^2} + \frac{b\operatorname{Re}\underline{Z}_X + jb\operatorname{Im}\underline{Z}_X + b^2}{\left|j\underline{Z}_X + b\right|^2} . \tag{17}$$

As it was told, the quasi-balance state of the analyzed circuit consists in the phase shift angle between distinguished signals $\underline{w}_1$ and $\underline{w}_2$ equal $-\pi/4$. The real and imaginary parts of the (17) are equal, respectively:

$$\operatorname{Re}\frac{\underline{w}_1}{\underline{w}_2} = \frac{b\operatorname{Re}\underline{Z}_X - b\operatorname{Im}\underline{Z}_X + b^2}{\left|j\underline{Z}_X + b\right|^2}, \tag{18}$$

and:

$$\operatorname{Im}\frac{\underline{w}_1}{\underline{w}_2} = \frac{-\left|\underline{Z}_X\right|^2 - b\operatorname{Re}\underline{Z}_X + b\operatorname{Im}\underline{Z}_X}{\left|j\underline{Z}_X + b\right|^2}. \tag{19}$$

Comparing (18) with (19), there is obtained:

$$b\operatorname{Re}\underline{Z}_X - b\operatorname{Im}\underline{Z}_X + b^2 = \left|\underline{Z}_X\right|^2 + b\operatorname{Re}\underline{Z}_X - b\operatorname{Im}\underline{Z}_X . \tag{20}$$

Hence:

$$\left|\underline{Z}_X\right|^2 = b^2 , \tag{21}$$

Finally the impedance modulus equation can be written in the form:

$$\left|\underline{Z}_X\right| = b . \tag{22}$$

If the circuit is used for the capacitance measurement, the equation expressing the approximate capacitance value can be written in the form:

$$\hat{C} = \frac{1}{\omega\left|\underline{Z}_X\right|} = \frac{1}{\omega b} . \tag{23}$$

## 4. VIRTUAL INSTRUMENT FOR MEASUREMENTS OF IMPEDANCE COMPONENTS

The measuring idea described by the block diagram (Fig. 2) was implemented in virtual instrument (Fig. 3). Measuring signals of the capacitor under test: the voltage drop, and the current transferred into voltage have been led to the acquisition card USB NI 6009. Next signal processing is made by the program written in graphic programming environment LabVIEW.

Basic blocks of the virtual instrument designed for the capacitance measurements are:

- The amplifier B of the settled gain. It forms the signal $U_B$ proportional to the current $\underline{I}_x$ flowing thorough the impedance under test,
- The phase shifter PF. It shifts the time course of the signal $U_A = \underline{U}_x$ by the angle 90° (it is equivalent to the multiplication by the imaginary unit $j$),
- The summing nodes. They generate the distinguished signals $\underline{w}_1$ and $\underline{w}_2$,
- The phase sensitive detector DF. It indicates the phase shift between distinguished signals $\underline{w}_1$ and $\underline{w}_2$.

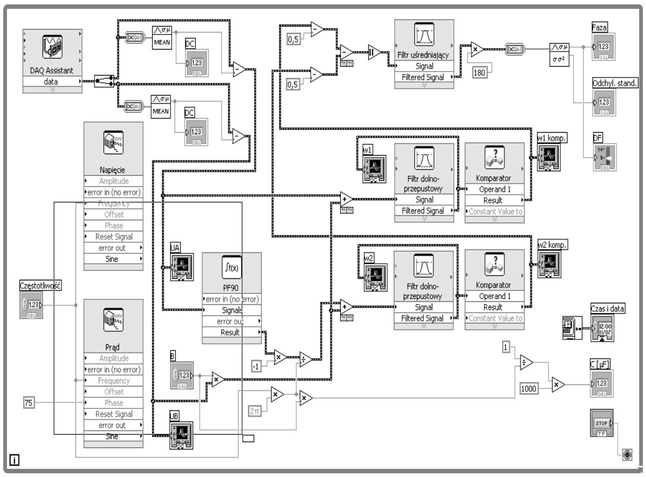


Fig. 3. The LabVIEW realization of the virtual capacitance meter.

## 5. MEASURING CIRCUIT TESTING

Most important module of the worked out virtual instrument is the phase sensitive detector, DF. This module is decisive for the measurement accuracy. A lot of different circuits commonly used for phase shift measurement were tested: circuits with pulse counters, circuits with the time to pulse height converter (TPHC), circuits with the time expander forming time to digital converters (TDC). In final circuit two different phase meters were checked to verify phase sensitive detection results.

The first solution of the phase meter is based on the dependence between the average value calculated for the instantaneous values of two voltage courses in the half period, and the phase shift value between time courses of the two voltages. This idea is easily adaptable in virtual instruments. The phase shift measurement of the sampled time courses must regard the sampling frequency, especially if the method is based on the averaging procedure.

The phase shift measurement accuracy based on this method depends on the averaging procedure (width of the averaging filter window). The standard deviation of the measured phase shift between two signals depends on the averaging window width, used for the averaging of instantaneous values of the signals (Tab. 1). It depends of course also on the sampling frequency.

If the averaging window width is increased (calculation basing on the larger sample number) the changes of the averaging filter output signal are smaller. In this case it must be noticed however, the latency time for resulting output signal of the averaging is longer. The choice of the optimal averaging window have to be based both on the sampling frequency of the compared signals, and theirs own frequency. Many tests of the virtual instrument were performed at measurement signal frequency changed in the range 10 Hz up to 100 Hz (standard frequency was 50 Hz). From results listed in the Tab. 1 it can be concluded the optimal averaging window width is 1 kS, for the frequency both 1 kS/s, and 10 kS/s. The difference consists in the result latency time. For the signals sampled with the frequency 10 kS/s the result appears as early as 0.1 s, but for the 1 kS/s it appears only just after 1 s.

Table 1. Dependence between measured phase standard deviation and the half-width of the moving averaging window for specified sampling frequency and measurement frequency 50 Hz.

| Half-width of the moving average window [sample] | Measured phase standard deviation [°] | |
|---|---|---|
| | Sampling frequency 1 kS/s | Sampling frequency 10 kS/s |
| 50 | 1.05 | 83.72 |
| 100 | 0.59 | 77.00 |
| 200 | 0.35 | 61.39 |
| 300 | 0.26 | 40.83 |
| 400 | 0.21 | 19.09 |
| 500 | 0.18 | 0.18 |
| 600 | 0.17 | 12.94 |
| 700 | 0.16 | 17.59 |
| 800 | 0.15 | 15.30 |
| 900 | 0.14 | 8.45 |
| 1000 | 0.13 | 0.13 |
| 2000 | 0.11 | 0.11 |
| 5000 | 0.09 | 0.10 |

The second solution of the phase meter used in the measuring circuit is based on the dual channel spectral measurement module (DCSM), which is accessible in the LabVIEW environment. The module may be used for the measurement of the phase shift existing between two signals of any shapes. The module works with specific frequency, depended on the sampling frequency of the compared signals. E.g. for the frequency 1 kS/s the spectrum range from 0 up to 500 Hz is analyzed, with the step 10 Hz.

The reading of the phase shift between two measured signals is essential when any phase meter of this kind is used. To improve this reading the function *Index Array* was used on the phase meter output. This function takes the content from the cell, addressed by the index. The index number is chosen on the base of the first harmonic signal frequency. This way of the phase measurement gives the right results, even if signals are distorted, and no preliminary filtering is used (no low pass filters at the input).

The phase shifter PF90 was realized as the circuit differentiating the sampled signal $U_B$. Such functionality is provided in the LabVIEW environment by the *Time Domain* module. It must be configured respectively, choosing the option *Continuous Calculation*.

Other parts of the worked out virtual instrument (amplifiers, filters, comparators) are realized basing on standard functions and structures of the graphic programming environment LabVIEW [3, 4].

## 6. CONCLUSIONS

The circuit presented in the paper is designated for capacitance measurement, basing on the impedance modulus measurement. It was realized as a virtual instrument using the acquisition card NI 6009, programmed in LabVIEW environment. Both the simulating tests and real RC object tests were performed with instrument. The structure of the program signal processing was left unchanged when the measuring signals were generated by the program, as well as when they were taken from real object under tests, supplied by the generator Agilent 33220A.

Both simulation results and experimental tests of real object confirmed the capacitance measurement possibility. The resolution 0.1 nF and the uncertainty less than 3% were achieved. The resolution of the measurement was determined by the input impedance of the acquisition card used for the experiment. Presented idea of the measurement is promising, and at this preliminary stage of the research can be regarded for further development. It is especially convenient for a virtual realization. Analyzed different phase detector realizations exhibited essential measurement uncertainty sources and allowed to configure optimally the measuring circuit modules. Next research is directed to the enlargement both the result resolution, and the frequency range of the measured signals, particularly at very low frequencies.

Preliminary tests of the presented circuit acknowledge the possibility of this virtual instrument idea implementation into impedance measurements of RC objects, of small loss angles. It can be also used in applications where very high accuracy is not needed, e.g. for insulation testing in very low frequency band, and where the use of other known instrument circuits (as e.g. bridges) is not convenient.

## REFERENCES


[1] M. A. Atmanand, V. J. Kumar and V. G. K. Murti: *A Microcontroler Based Quasi-Balanced Bridge for the Measurement of L, C and R*. IEEE Transactions on Instrumentation and Measurement, vol. 45, no. 3, June 1996, pp. 757-761.

[2] M. I. Burbelo: *Universal quasi-balanced bridges for measuring the parameters of four-element two-terminal networks*. Izmeritel'naya Tekhnika, vol. 44, no.11, Nov. 2001, pp.1130-3.

[3] *LabVIEW Fundamentals*. National Instruments Corporation 2005.

[4] P. Bobiński, W. Winiecki: *Development Environment for Distributed Measurement and Control Systems*. Measurement Automation and Monitoring, vol. 53, no. 9bis, 2007, pp. 698-701.

[5] A. Cichy, A. Skórkowski: *A. Cichy, A. Skórkowski: Virtual quasi-balanced circuit for the loss factor measurement*. Measurement Automation and Monitoring, vol. 54, no. 2, 2008, pp. 48-51.

[6] A. Cichy, A. Skórkowski: *Virtual realization of a quasi-balanced circuit for measuring the dielectric condition index of capacitance type*. Measurement Automation and Monitoring, vol. 55, no. 1, 2009, pp. 34-37.


The paper has been supported by grant No. 505 002 32/0199